Cumhuriyet Science Journal

e-ISSN: 2587-246X
ISSN: 2587-2680

Cumhuriyet Sci. J., 42(2) (2021) 476-492
http://dx.doi.org/10.17776/csj.680516

Computational analysis of optical trapping of transparent and reflecting micron-sized spherical particles

Ufuk PARALI [1, *]

[1] *KalyonPV Research and Development Center, Kalyon Güneş Teknolojileri Üretim A.Ş., 06909, Ankara / TURKEY*

Abstract

In the ray-optics regime, we calculated the radial and axial force field on a micron-sized spherical particle in an optical levitation trap. The momentum change in the photon-stream path of tightly focused incident laser beam causes the calculated force field in the optical trap. The computational results for the force field are compared with the literature and a good agreement is obtained. Utilizing the benchmarked force field, the optical trapping dynamics of (i) a transparent spherical particle with continuous-wave TEM_{00} Gaussian beam and (ii) a reflecting spherical particle with continuous-wave TEM_{01}^{*} Laguerre-Gaussian beam under various conditions are simulated in Matlab.

Article info

History:
Received: 27.01.2020
Accepted: 20.05.2021

Keywords:
Optical trapping,
Gaussian beam,
Laguerre-Gaussian beam,
Micron-sized particle.

1. Introduction

Trapping and precisely manipulating micron and sub-micron scale objects without interfering with a physical attachment is an interesting technical challenge. In the early 1970s, Ashkin and colleagues have reported the first applicable observation of acceleration and trapping of particles by radiation forces [1-6]. The technique opened the door to the study of the dynamics of single suspended particles, molecules, biological cells, and water droplets held in an optical levitation trap and to completely isolate these objects from their immediate surroundings [7, 8]. Thus, using radiation forces obtained by tightly focusing laser beams has become a useful tool for trapping and manipulating micrometer-sized particles in many scientific areas such as chemistry, physics and biology [2,3,9-15]. There are three different approaches for deriving the theoretical expressions for radiation forces due to laser beam exposures; (i) the electromagnetic dipole model that calculates the radiation force for particles in the Rayleigh regime where the objects are much smaller than the wavelength of the laser beam, and (ii) the ray-optics approach which has been first studied by Ashkin and applicable to the objects larger than the wavelength of the laser beam used in optical levitation trap [2,7,16-20]. Especially the single-beam gradient trap setups were originally designed for Rayleigh particles [2,5,21]. These setups are also named as optical tweezers which has been experimentally shown that they could be used for trapping and manipulating micron-sized biological particles such as living cells and organelles within living cells [2,3,6,22]. In 2018, Ashkin won the Nobel Prize for his contributions to the optical tweezers and their application to biological systems. (iii) The third approach for the mathematical definition of the radiation force is the Lorenz-Mie model which has been used for the objects with dimensions close to the wavelength of the tightly focused laser beam utilized in optical trap setup [23]. Recently, the studies on the optical levitation of sub-micron particles are

being focused on trapping by ultrashort laser pulses [24,25] high precision nano-g acceleration sensing [26,27] manipulation of the trapped sub-micron particles and applications in optomechanics [28,29].

There are unique design requirements for an optical levitation trap setup. Especially regarding stability, loading of targets under vacuum and trapping of transparent or reflective targets, a computational tool requirement to help inform further development and experimental considerations motivate the work we present here. In this work, we focused on Ashkin's approach of ray-optics model [1-6] and computationally analysed the optical trapping of transparent and reflecting micron-sized spherical particles. This paper gives the computational results of (i) optical trapping of a transparent spherical particle with continuous-wave TEM_{00} Gaussian beam, and (ii) optical trapping of a reflecting spherical particle with continuous-wave TEM_{01}^{*} Laguerre-Gaussian beam under various conditions. Both the evolution of axial

*Corresponding author. *e-mail address: uparali@kalyonpv.com*

and radial dynamics are calculated in Matlab utilizing Velocity Verlet integrator algorithm.

The rest of this paper is organised as follows; Section 2 gives the analytical model and the simulation results for optical trapping of transparent spherical particle with TEM_{00} Gaussian beam. The benchmarking process for the developed Matlab code is explained in this part. Section 3 describes the analytical model for optical trapping of reflecting spherical particle with TEM_{01}^{*} Laguerre-Gaussian beam and gives the simulation results. The conclusion and the proposed future work is explained in Section 4. In Appendix, the Matlab modules developed in this study are given.

2. Optical Trapping of Transparent Micron-sized Spherical Particle with TEM_{00} Gaussian Beam

In this study, the equations for the axial and radial force fields of the ray-optics model have been utilized from Gauthier et al. [7]. We calculated and simulated the force fields on a micron-sized transparent spherical particle due to TEM_{00} Gaussian beam exposure using Matlab. In Section 2.1, the results for the benchmarking of the developed Matlab code is given. Once the force fields are obtained correctly, using Velocity Verlet algorithm in Section 2.2, we simulated the evolution of the axial position, radial position and radial velocity of the particle trapped in TEM_{00} Gaussian beam as shown in Figure 1 below.

Due to the change in the momentum of the photon-stream while passing through the transparent micron-sized spherical particle, a net force occurs on the particle as shown in Figure 1a. Here, particle has an inital radial offset with respect to the center of the Gaussian beam. Under the exposure of this force, particle departs towards the centre of the Gaussian beam. Once it reaches the center of the beam, the transverse force diminishes and only the longitudinal force in the direction of the Gaussian beam remains (see Figure 1b). Here, the transverse direction is on the radial axis and the longitudinal direction is on the propagation direction of the beam which is assumed to be on the z-dimension (see Figure 1c). Due to the viscosity effect, the transparent spherical particle will have damped oscillation in the transverse direction at the vicinity of the center of the beam as depicted in Figure 1c. Here, the comparison for the trapping of transparent and reflecting particles are also shown in Figure 1c. The difference between the trapping dynamics of transparent and reflecting spherical particle is that; while trapping a transparent spherical with TEM_{00} mode is possible, for trapping reflecting spherical particle TEM_{01}^{*} mode is needed. In order to trap a reflecting particle with TEM_{01}^{*} mode, the particle must be located somewhere in the 2nd and the 3rd regions of the beam. In these regions, reflecting particle will have a damped oscillation just as similar to the transparent particle having a damped oscillation under TEM_{00} mode exposure as shown in Figure 1c.

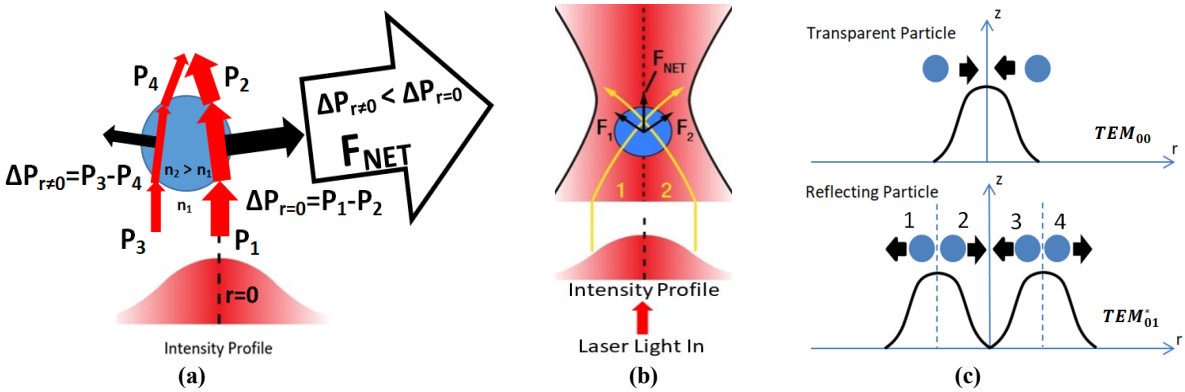

Figure 1. (a) Ray-optics approach of the photon-stream path incident upon the lower side of a transparent spherical particle with an arbitrarily given initial radial offset with respect to the center axis of the Gaussian beam. Here, $\Delta P_{r=0}$, $\Delta P_{r\neq0}$, n_1 and n_2 denotes for the momentum change at r=0, momentum change at r≠0, ambient refractive index and particle refractive index, respectively. **(b)** Transparent spherical particle located in the center of a Gaussian beam [30]. **(c)** Comparison of trapping transparent spherical particle with TEM_{00} Gaussian beam and trapping reflecting spherical particle with TEM_{01}^{*} Laguerre-Gaussian beam. It is not possible to trap a reflecting particle with TEM_{00} mode.

For the trapping simulations of the transparent spherical particle, we must explicitly define the intensity of the TEM_{00} Gaussian beam in the numerical model. It is defined as:

$$I(\rho,z) = \frac{2P}{\pi W(z)^2} exp\left[\frac{-2\rho^2}{W(z)^2}\right] \quad (1)$$

where; **(i)** ρ is the radial displacement of a point on the surface of the spherical particle (not the center of the

particle) (see Figures 2a and 2b). If the center of the spherical particle is displaced from the center of the beam by $\bar{a}$, then we can write the radial displacement (with respect to the global coordinate system) of a point on the sphere as $\bar{d}$. Therefore, the magnitude of the radial displacement is defined as ρ. In other words, ρ is the radial distance from the beam's axis. From Figures 2a and 2b, we can write;

$$\bar{d} = \rho\hat{d} \tag{2}$$

where $\rho = |\bar{d}|$. Here, $\bar{d}$ is the position of points on the surface of the spherical particle with respect to the global coordinate system. Thus looking at Figures 2a and 2b, the following can be written;

$$\bar{a} = a_x\hat{a}_x + a_y\hat{a}_y + a_z\hat{a}_z \tag{3}$$

and

$$\bar{b} = x\hat{a}_x + y\hat{a}_y + z\hat{a}_z \tag{4}$$

where $\bar{a}$ is the position of the center of the spherical particle with respect to the global coordinate system. Here, $x = RSin\theta Cos\emptyset$ and $y = RSin\theta Sin\emptyset$. Using $\bar{a}$ and $\bar{b}$, we can write

$$\bar{d} = \bar{a} + \bar{b}. \tag{5}$$

Assume $a_y = 0$ and $a_z = 0$. Thus,

$$\bar{d} = (a_x + x)\hat{a}_x + y\hat{a}_y \tag{6}$$

and

$$\rho = |\bar{d}| \rightarrow \rho = \sqrt{\bar{d}\bar{d}}, \tag{7}$$

$$\rho = (a_x^2 + 2a_x x + x^2 + y^2)^{1/2}. \tag{8}$$

Here, we can define ρ as:

$$\rho = [a_x^2 + 2a_x RSin\theta Cos\emptyset + (RSin\theta Cos\emptyset)^2 + (RSin\theta Sin\emptyset)^2]^{1/2} \tag{9}$$

where $\theta \in [0, \pi/2]$ and $\emptyset \in [0, 2\pi]$.

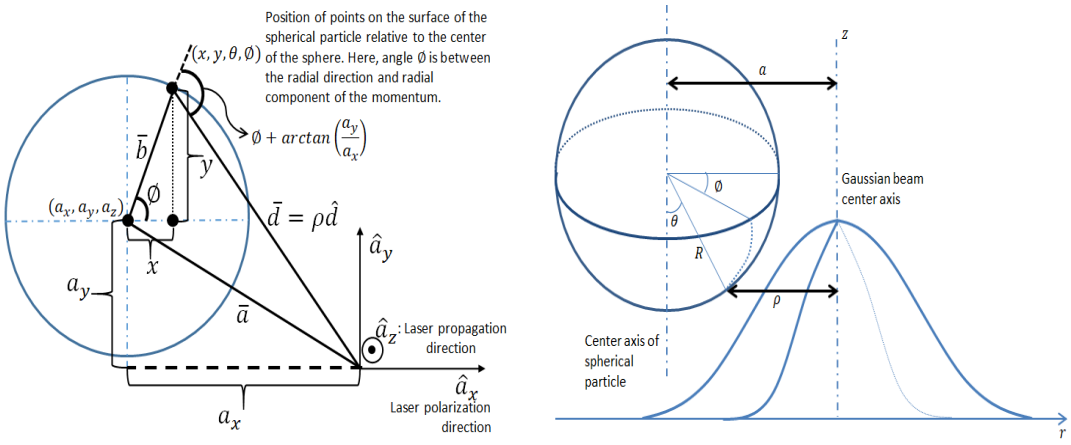

Figure 2. (a) 2-dimensional view of the spherical particle from the above. Here, the propagation of the Gaussian beam is at $\hat{a}_z$ direction. **(b)** 3-dimensional view of a spherical particle under the exposure of a TEM_{00} Gaussian beam. Particle has an arbitrary initial radial offset with respect to the center axis of the beam. Here, $\emptyset$ is the polar angle, θ is the incident angle and $|\bar{a}|$ is the radial distance between the center axis of the beam and center axis of the sphere [8].

(ii) z is the vertical displacement of a point on the surface of the spherical particle (not the center of the particle). In other words, it is the distance measured along the beam's direction of propagation with $z = 0$ located at the minimum waist;

$$z = a_z - RCos\theta \tag{10}$$

(iii) P is the total power of the laser beam and $w(z)$ is the beam width defined as:

$$w(z) = w_0\left[1 + \left(\frac{z}{z_0}\right)^2\right]^{1/2} \tag{11}$$

where w_0 is the beam waist and z_0 is the Rayleigh range defined as $z_0 = {\pi w_0}^2/\lambda_0$ where λ_0 is the wavelength of the laser beam.

2.1. Benchmarking the Matlab code by comparing force plots

There is a vast amount of literature on optical trapping codes containing force plots of the optical gradient forces. As mentioned above, in this study, the equations for the axial and radial force fields of the ray-

optics model have been utilized from Gauthier et al. [7]. Thus, in order to validate our optical force modules of the Matlab code are functioning correctly, the Matlab outputs of our code are compared with the results of [7]. In the benchmarking simulations, three cases were tested and compared in which the radius of the spherical particle is (i) smaller than the beam waist, (ii) equal to the beam waist and (iii) larger than the beam waist as shown in Figure 3 below. For a correct comparison of the results in the benchmarking process, the physical parameters of [7] are utilized as listed in Table 1 below. In the next section, dynamic viscosity, refractive index of the spherical particle, wavelength of the beam and the laser power are changed.

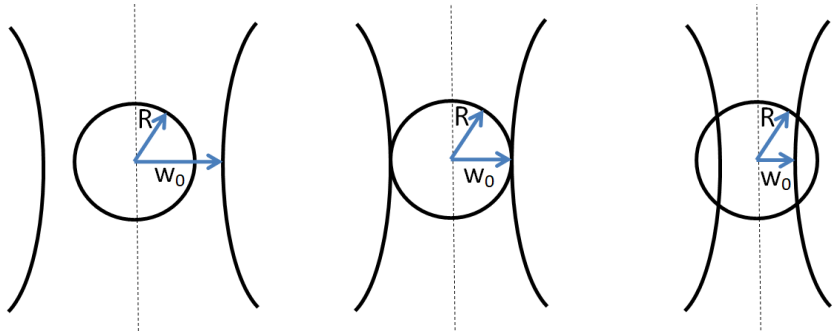

(a) **(b)** **(c)**

Figure 3. (a) Radius of spherical particle is smaller than laser beam waist ($R<w_0$). **(b)** Radius of spherical particle is equal to laser beam waist ($R=w_0$). **(c)** Radius of spherical particle is larger than laser beam waist ($R>w_0$).

Table 1. Values of the parameters utilized from Gauthier et al. [7] for code benchmarking calculations.

Input Parameters	Value
Initial radial offset (m)	0
Initial axial offset (m)	0 (for Figures 4-b, 4-d and 4-f)
Initial axial offset (m)	$(0\text{-}25\text{-}50\text{-}100)\times10^{-6}$ (for Figures 4-h and 4-j)
Particle radius (m)	$(1.5\text{-}2\text{-}2.5)\times10^{-6}$
Beam waist (m) – FWHM	2×10^{-6}
Laser power (mW)	20
Density of the particle (kg/m^3)	1197.2
Medium dynamic viscosity ($kgm^{-1}s^{-1}$)	1.8×10^{-7} (=18 μPa.sec)
Laser wavelength (nm)	514
Ambient refractive index – n_1	1.333
Particle rrefractive index – n_2	1.5568

Looking at Figure 4 below, a good agreement is seen between the force curves acting as a sanity check against our Matlab code. In the Appendix, the related Matlab modules implemented in the benchmarking calculations are provided.

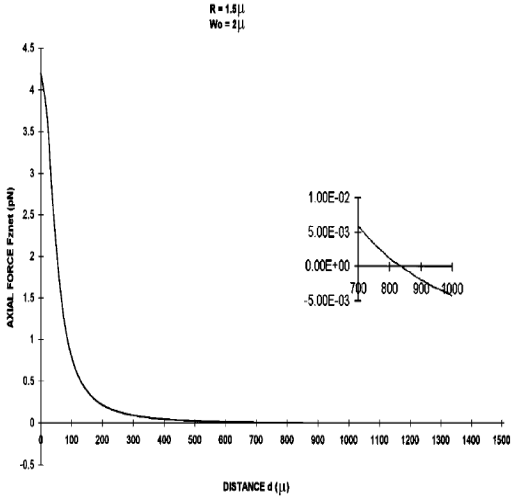

(a)

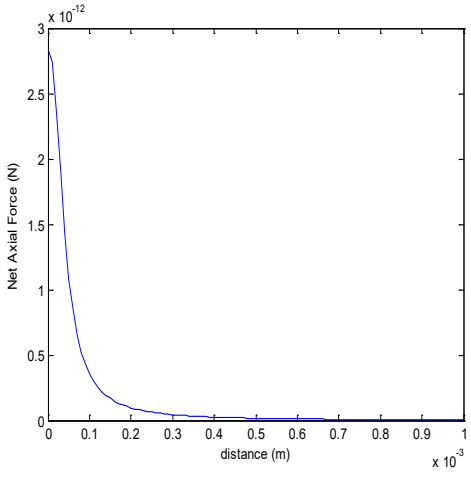

(b)

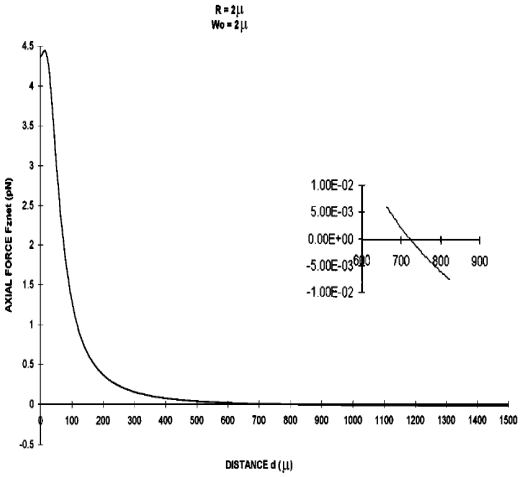
R = 2μ
Wo = 2μ
AXIAL FORCE Fznet (pN)
DISTANCE d (μ)

(c)

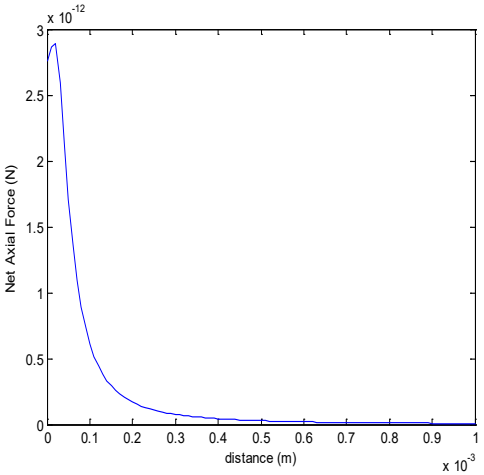
x 10^-12
Net Axial Force (N)
distance (m)
x 10^-3

(d)

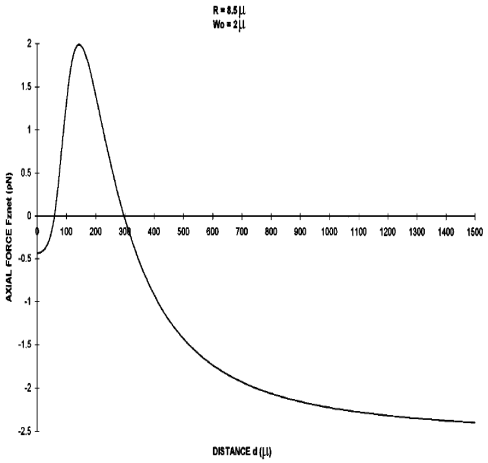
R = 8.5μ
Wo = 2μ
AXIAL FORCE Fznet (pN)
DISTANCE d (μ)

(e)

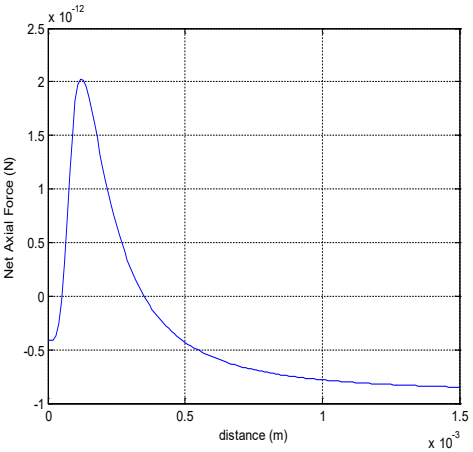
x 10^-12
Net Axial Force (N)
distance (m)
x 10^-3

(f)

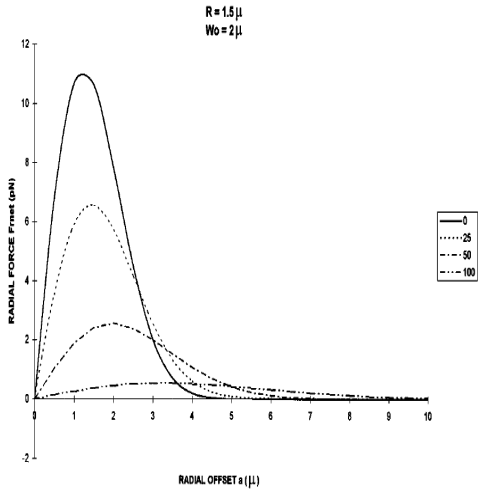
R = 1.5μ
Wo = 2μ
RADIAL FORCE Frnet (pN)
RADIAL OFFSET a (μ)
0
25
50
100

(g)

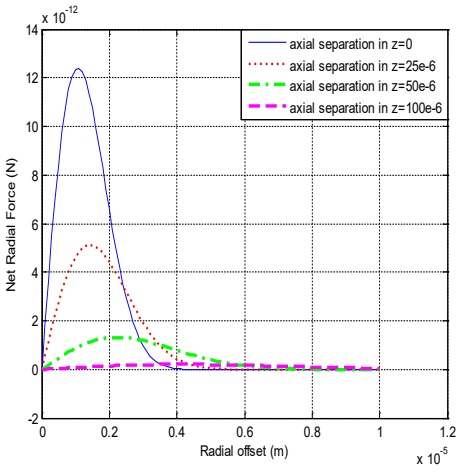
x 10^-12
Net Radial Force (N)
Radial offset (m)
x 10^-5
axial separation in z=0
axial separation in z=25e-6
axial separation in z=50e-6
axial separation in z=100e-6

(h)

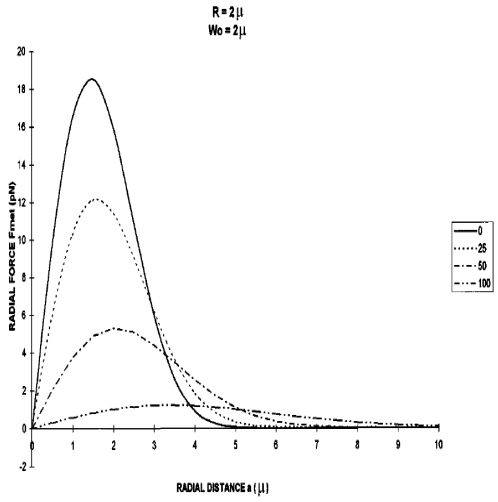

(i)

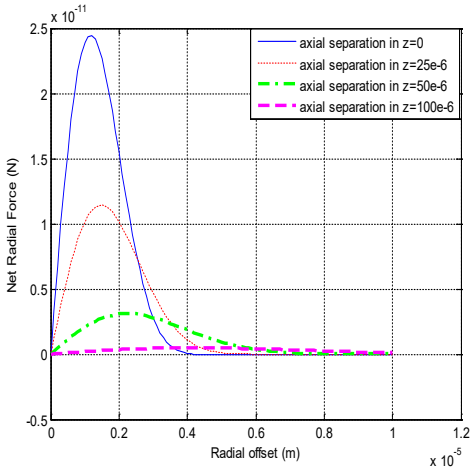

(j)

Figure 4. (a) Evolution of axial force with axial distance from beam waist for R=1.5μm (radius of transparent spherical particle) and w_0=2μm (laser beam waist) [7]. **(b)** Corresponding Matlab output of our code for Fig. 3-a (R=1.5μm, w_0=2μm). **(c)** Evolution of axial force with axial distance from beam waist for R=2μm and w_0=2μm [7]. **(d)** Corresponding Matlab output of our code for Fig. 3-c (R=2μm, w_0=2μm). **(e)** Evolution of axial force with axial distance from beam waist for R=8.5μm and w_0=2μm [7]. **(f)** Corresponding Matlab output of our code for Fig. 3-e (R=8.5μm, w_0=2μm). **(g)** Evolution of radial force with radial distance from beam axis for R=1.5μm and w_0=2μm [7]. **(h)** Corresponding Matlab output of our code for Fig. 3-g (R=1.5μm, w_0=2μm). **(i)** Evolution of radial force with radial distance from beam axis for R=2μm and w_0=2μm [7]. **(j)** Corresponding Matlab output of our code for Fig. 3-i (R=2μm, w_0=2μm).

2.2. Simulation results for optical trapping of transparent spherical micro-particle

Once the credibility of the code was established proving the force fields are being calculated properly, as the next step we move forward to investigate the dynamics of the transparent spherical particle under *TEM*$_{00}$ Gaussian beam exposure. Thus, in order to understand the evolution of the axial and radial dynamics of the particle in the optical trap, we utilized the Velocity Verlet (VV) algortihm in side the code. It is a popular integrator giving pricesly the velocity and the position of the particle at the same time t in a three-stage calculation [31]:

$$V\left(t_0+\frac{\Delta t}{2}\right)=V(t_0)+\frac{\Delta t}{2}\frac{F(r(t_0),t_0)}{m} \quad (12)$$

$$r(t_0+\Delta t)=r(t_0)+\Delta t V\left(t_0+\frac{\Delta t}{2}\right) \quad (13)$$

$$V(t_0+\Delta t)=V\left(t_0+\frac{\Delta t}{2}\right)+\frac{\Delta t}{2}\frac{F(r(t_0+\Delta t),t_0+\Delta t)}{m} \quad (14)$$

Here, F is the force field (Lorentz force) on the particle. It must be noted that F is being calculated twice in the VV algorithm. The first evaluation of F is at the inital time and position of the particle (see Eq. 12). The second evaluation of F is at the next position of the particle after the time-step Δt (see Eq. 14) [31].

In the simulations, we utilized the following values for the given parameters in Table 2 below:

Table 2. Values of the parameters used in the simulations of optical trapping dynamics of transparent spherical particle.

Input Parameters	Value
Initial radial offset (m)	$1x10^{-6}$
Initial axial offset (m)	$-5x10^{-3}$
Initial axial velocity (ms^{-1})	5.0
Particle radius (m)	$5x10^{-6}$
Beam waist (m) – FWHM	$4x10^{-6}$
Laser power (mW)	200
Density of the particle (kg/m^3)	2500
Medium dynamic viscosity ($kgm^{-1}s^{-1}$)	$1.82x10^{-6}$
Laser wavelength (nm)	532
Simulation step size (sec) – Δt	$5x10^{-5}$
Ambient refractive index – n_1	1.0
Particle refractive index – n_2	1.52

The simulation results for the evolution of the axial and radial trajectories of the transparent spherical particle in the optical trap are given in Figure 5 below. In the Appendix, the related Matlab modules implemented for these simulations are provided. For a proper experimental design of an optical trap, it is vital to understand the axial and radial dynamics of a particle located in the optical trap. Thus having a computational tool providing the evolution of particle trajectory is extremely beneficial for the experimentalists working in this research field.

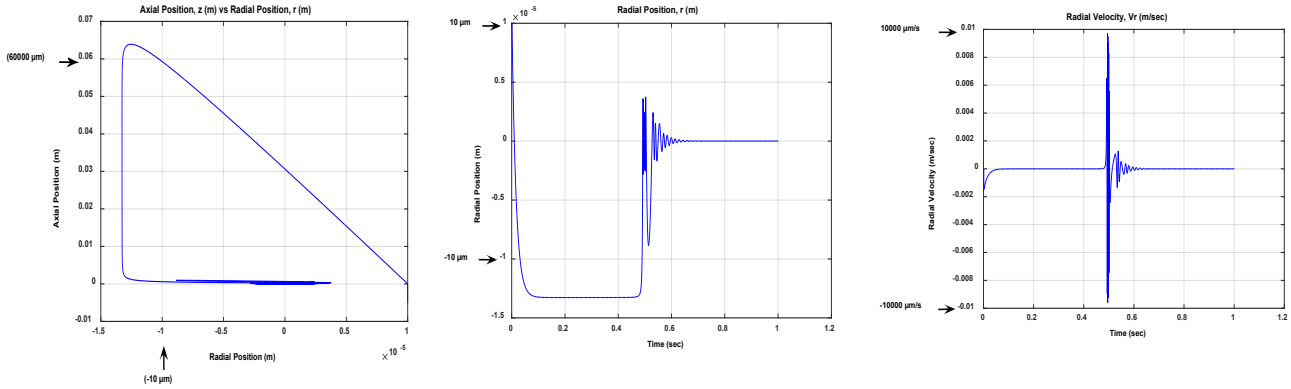

(a) (b) (c)

Figure 5. (a) Radial vs axial trajectory of the particle under *TEM₀₀* beam exposure in the optical trap. **(b)** Temporal evolution of the damped oscillation of the particle at the vicinity of the center axis of the *TEM₀₀* laser beam. **(c)** Temporal evolution of the radial velocity of the particle in the optical trap.

3. Optıcal Trapping Of A Reflecting Particle Under TEM_{01}^{*} Laguerre-Gaussıan Beam

As explained in Section 2, different than trapping a transparent particle with a *TEM₀₀* beam, we need TEM_{01}^{*} Laguerre-Gaussian beam for trapping a reflecting spherical particle. In this section, first the derivation of the intensity expression of Laguerre-Gaussian donut beam in terms of total beam power is discussed. Laguerre-Gaussian beams are the higher-order Gaussian beams in cylindrical coordinates [32,33]:

$$E_{p,l}(\rho,\theta,z)=\frac{A_{p,l}}{w(z)}\left(\frac{\sqrt{2}\rho}{w(z)}\right)^{l}L_p^{l}\left(\frac{2\rho^2}{w(z)}\right)\exp\left(\frac{-\rho^2}{w(z)^2}\right)\exp\left(\frac{ik\rho^2}{2R(z)}\right)\exp(i[l\theta-\varphi(z)]) \quad (15)$$

where $\rho=(x^2+y^2)^{1/2}$, $\theta=tan^{-1}\left(y/x\right)$, $w(z)$ is the beam width defined same as the Gaussian beam width, L_p^{l} is the associated Laguerre polynomial of radial order p and azimuthal order l and $A_{p,l}$ is the constant term for normalizing the beam equation [34]:

$$A_{p,l}=p!\left(\frac{2}{\pi p!(|l|+p)!}\right)^{1/2}. \quad (16)$$

Here, if $l\neq 0$ and $p=0$, then the beams have a characteristic single-ringed donut. The radius of donut is proportional to $l^{1/2}$. Thus, $LG_0^1|_{(p=0,l=1)}=TEM_{01}^{*}$ [33-35]. For LG_p^l mode, the amplitude expression can be defined from Eq. 15 as below [32,33,35]:

$$Eo_{p,l}(\rho,\theta,z)=\frac{A_{p,l}}{w(z)}\left(\frac{\sqrt{2}\rho}{w(z)}\right)^{l}L_p^{l}\left(\frac{2\rho^2}{w(z)}\right)\exp\left(\frac{-\rho^2}{w(z)^2}\right) \quad (17)$$

Using Eq. 17, the intensity expression of the donut mode can be derived [35]:

$$I_{LG_0^1}=\frac{c\varepsilon_o}{2}\left(Eo_{p=0,l=1}\right)^2, \quad (18)$$

$$I_{LG_0^1}=\frac{c\varepsilon_o}{2}\left[\frac{A_{p=0,l=1}}{w(z)}\left(\frac{\sqrt{2}\rho}{w(z)}\right)^{1}L_0^{1}\left(\frac{2\rho^2}{w(z)}\right)\exp\left(\frac{-\rho^2}{w(z)^2}\right)\right]^2 \quad (19)$$

where

$$A_{p=0,l=1}=\left[p!\left(\frac{2}{\pi p!(|l|+p)!}\right)^{1/2}\right]_{p=0,l=1}, \quad (20)$$

$$A_{p=0,l=1}=\sqrt{\frac{2}{\pi}}, \quad (21)$$

and

$$L_0^{1}\left(\frac{2\rho^2}{w(z)}\right)=1 \text{ where } L_0^{l}(x)=1. \quad (22)$$

Using Eqs. 21 and 22 in Eq. 19, we can get:

$$I_{LG_0^1}=\frac{c\varepsilon_o}{2}\left[\frac{\sqrt{2/\pi}}{w(z)}\left(\frac{\sqrt{2}\rho}{w(z)}\right)\exp\left(\frac{-\rho^2}{w(z)^2}\right)\right]^2, \quad (23)$$

$$I_{LG_0^1}=(2c\varepsilon_0)\left[\frac{1}{\pi w(z)^4}\rho^2 exp\left(\frac{-2\rho^2}{w(z)^2}\right)\right]. \quad (24)$$

The total optical power carried by the beam is the integral of the optical intensity over a transverse plane as $P=\int_0^{\infty} I(\rho,z)\,2\pi\rho d\rho$ [34,35].

Thus using Eq. 24, the total power can be written as [33-35]:

$$P=\frac{2c\varepsilon_0}{\pi w(z)^4}\int_0^{\infty}\rho^2 exp\left(\frac{-2\rho^2}{w(z)^2}\right)2\pi\rho d\rho, \quad (25)$$

$$P=\frac{4c\varepsilon_0}{w(z)^4}\int_0^{\infty}\rho^3 exp\left(\frac{-2\rho^2}{w(z)^2}\right)d\rho. \quad (26)$$

The definition of the integral term in Eq. 26 is defined as [36]:

$$\int_0^\infty x^n exp(-ax^2)dx = \begin{cases} (i)\ \frac{1}{2}\Gamma\left(\frac{n+1}{2}\right)\Big/_{a^{n+1}/_2}; (n > -1, a > 0) \\ (ii)\ \frac{(2k-1)!!}{2^{k+1}a^k}\sqrt{\frac{\pi}{a}}; (n = 2k, k\ is\ integer, a > 0, \\ \qquad\qquad !!\ is\ double\ factorial) \\ (iii)\ \frac{k!}{2a^{k+1}}; (n = 2k+1, k\ is\ integer, a > 0) \end{cases} \quad (27)$$

The integral term in Eq. 26 ($n = 3$, $k = 1$ and $a = \frac{2}{w(z)^2} > 0$) satisfies both of the conditions for (i) and (iii). For the value of the integral term, we found the same results:

$$(i) \quad \frac{\frac{1}{2}\Gamma(2)}{\left(\frac{2}{w(z)^2}\right)^2} = \frac{w(z)^4}{8}, \quad (28)$$

and

$$(iii) \quad \frac{1!}{2\left(\frac{2}{w(z)^2}\right)^2} = \frac{w(z)^4}{8}. \quad (29)$$

This result can be used in Eq. 26 for defining P :

$$P = \frac{4c\varepsilon_0}{w(z)^4}\frac{w(z)^4}{8}, \quad (30)$$

$$P = \frac{c\varepsilon_0}{2}. \quad (31)$$

Using Eq. 31 in Eq. 24, the intensity expression of the donut mode in terms of power can be written as:

$$I_{LG_0^1} = TEM_{01}^* = \frac{4P}{\pi w(z)^4}\rho^2 exp\left(\frac{-2\rho^2}{w(z)^2}\right). \quad (32)$$

3.1. Simulation results for optical trapping of reflecting spherical micro-particle

Utilizing Eq. 32, the axial optical trapping dynamics of micron-sized reflecting spherical particles with various radius values and with various initial axial positions are simulated. The following parameters in Table 3 are used in the simulations. The results are depicted in Figures 6 and 7 below.

Table 3. Values of the parameters used in the simulations of optical trapping dynamics of reflecting spherical particle.

Input Parameters	Value
Initial radial offset (m)	0
Initial axial offset (m)	(200 and -50)x10^{-6}
Initial axial velocity (m/sec)	0
Particle radius (m)	(2 - 2.5 - 3.5)x10^{-6}
Beam waist (m) – FWHM	3x10^{-6}
Laser power (mW)	600
Density of the particle (kg/m^3)	1197.2
Medium dynamic viscosity (kgm^{-1}sec^{-1})	1.82x10^{-5}
Laser wavelength (nm)	532
Simulation step size (sec) – Δt	1x10^{-5}

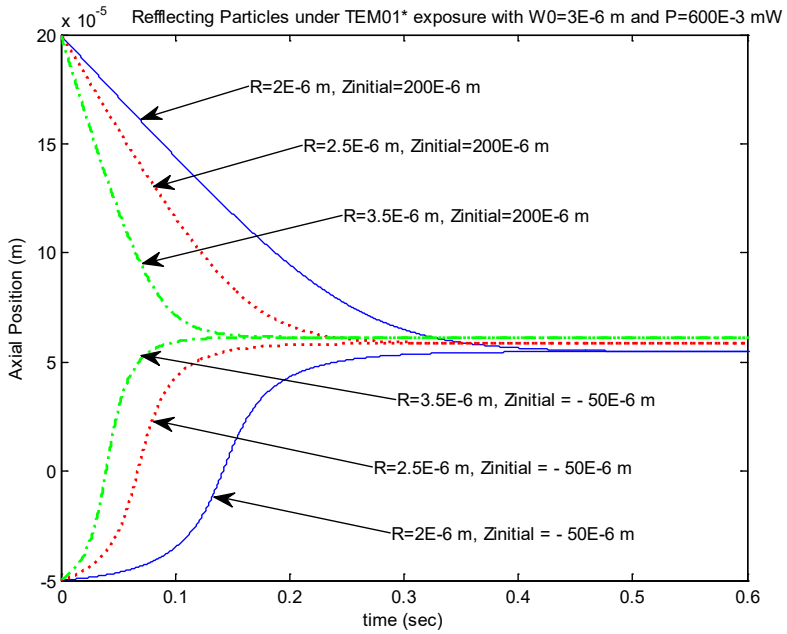

Figure 6. The axial stabilization of the particles with different radius (R) values and initial axial positions (Zinitial).

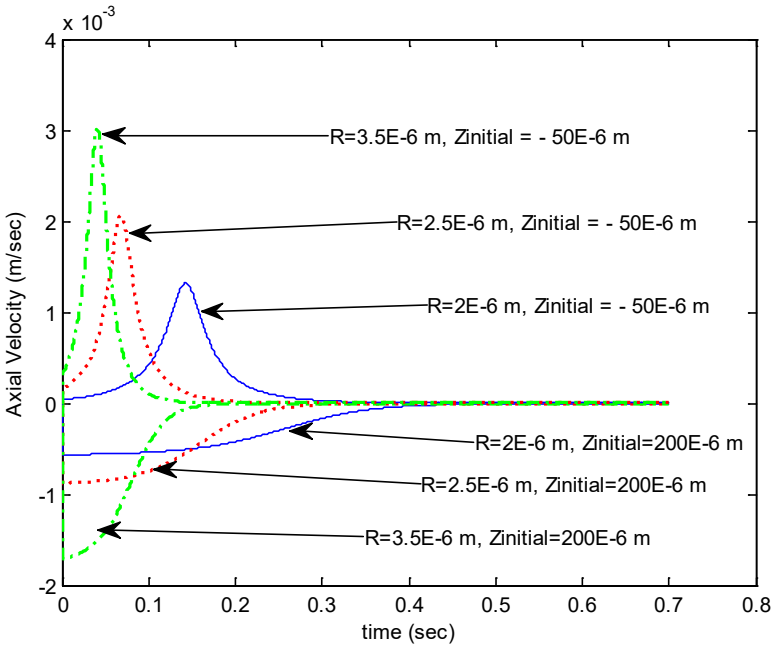

Figure 7. The axial velocity of the particles with different radius (R) values and initial axial positions (Zinitial).

4. Conclusion and Future Work

The momentum change in the photon-stream path of incident laser beam causes radiation force field. Using this radiation force field for trapping and manipulating micron-sized particles by tightly focusing laser beams in an optical trap has become a useful tool for many recent research areas. Due to the unique design requirements in an optical trap experiment, a computational tool is required for a better setup development. In this work, using Ashkin's approach of ray-optics model, we computationally analysed the optical levitation trapping of transparent and reflecting micron-sized spherical particles. We calculated the radiation force field using continuous-wave TEM_{00} Gaussian and TEM_{01}^{*} Laguerre-Gaussian laser beams for the optical trapping of transparent and reflecting particles, respectively. Utilizing Velocity Verlet algorithm, evolution of optical levitation trap dynamics are analysed in Matlab. As a future challenging work,

we aim to focus on analytical modelling and simulation of optical trapping of micron-sized metamaterials having negative index of refraction.

Appendix

A.1. Matlab code for the benchmarking process and optical trapping simulations of the transparent spherical micro-particle

This section gives the Matlab functions developed for both benchmarking process and optical trap simulations. Figure 8 below gives the geometric model of the photon-stream path of the incident beam on a transparent spherical particle where the refractive index of the particle is greater than the refractive index of the ambient. During calculating the force field on the particle, we took into consideration the momentum change due to the 1st reflected & transmitted beams and 2nd reflected & transmitted beams in this ray-optics model.

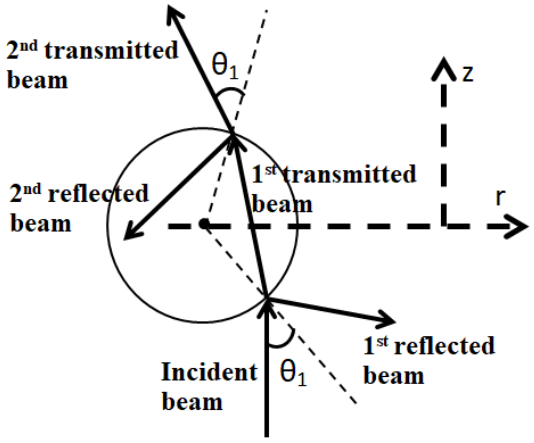

Figure 8. Reflected and transmitted ray-optics model of a transparent spherical particle under the exposure of a laser beam. The force due to the momentum change with respect to the 1st reflected & transmitted beams and 2nd reflected & transmitted beams are calculated in the given Matlab modules below. Using the calculated force-fields, the trap dynamics of the particle is simulated.

```
function f=forceAxial()
% Written by Ufuk Paralı
% This function calculates (within the geometrical optics regime) the total axial force
% on a transparent spherical particle in the optical trap due to the 1st reflected and
% 1st transmitted photon-stream paths and 2nd reflected and 2nd transmitted photon-
% stream paths of a continuous-wave TEM00 Gaussian laser beam.
global az
global ax
global R
global W0
global P
global n0
global ns
global lambda0
ax=0; % Initial radial offset of particle from center axis of laser beam
R=2e-6; % Radius of spherical particle
W0=1.5e-6; % Beam waist
P=20e-3; % Laser power
n0=1.333; % Refractive index of ambient
ns=1.5468; % Refractive index of transparent spherical particle
lambda0=514e-9; % Laser wavelength - m
density=1000; % Particle density - kg/m^3
m=density*(4/3)*pi*R^3; % mass of the spherical particle - kg
g=9.8; % m/s^2
ForceWeight=m*g;
counter=1; % counter initialization

for az=0:1e-5:5e-3
  posAxial(counter)=az; % Axial position of the particle in the trap
  % Axial force due to the 1st reflected photon-stream path

ForceOneRZ=dblquad(@forceOneReflectedZ,0,2*pi,0,pi/2);

  % Axial force due to the 1st transmitted photon-stream path

ForceOneTZ=dblquad(@forceOneTransmittedZ,0,2*pi,0,pi/2);

  % Axial force due to the 2nd reflected photon-stream path
```

```
ForceTwoRZ=dblquad(@forceTwoReflectedZ,0,2*pi
,0,pi/2);

   % Axial force due to 2nd transmitted photon-stream
path

ForceTwoTZ=dblquad(@forceTwoTransmittedZ,0,2*
pi,0,pi/2);

   % Total axial force on the particle

ForceAxial(counter)=ForceOneRZ+ForceOneTZ+For
ceTwoRZ+ForceTwoTZ-
   ForceWeight;
   counter=counter+1;
end
plot(posAxial,ForceAxial)
grid on
return

function f=forceRadial()
% Written by Ufuk Paralı
% This function calculates (within the geometrical
optics regime) the total radial force
% on a transparent spherical particle in the optical trap
due to the 1st reflected and
% 1st transmitted photon-stream paths and 2nd
reflected and 2nd transmitted photon-
% stream paths of a continuous-wave TEM00
Gaussian laser beam.
global az
global ax
global R
global W0
global P
global n0
global ns
global lambda0
az=0; % Initial axial offset of the particle in the trap
R=2e-6; % Radius of spherical particle
W0=1.5e-6; % Beam waist
P=20e-3; % Laser power
n0=1.333; % Refractive index of ambient
ns=1.5468; % Refractive index of transparent spherical
particle
lambda0=514e-9; % Laser wavelength - m
counter=1; % counter initialization
for ax=0:1e-7:10e-6;
   posRadial(counter)=ax; % Radial position of the
particle in the trap
   % Radial force due to the 1st reflected photon-
stream path
   ForceOneRR=-
dblquad(@forceOneReflectedR,0,2*pi,0,pi/2);

   % Radial force due to the 1st transmitted photon-
stream path
   ForceOneTR=-
dblquad(@forceOneTransmittedR,0,2*pi,0,pi/2);

   % Radial force due to the 2nd reflected photon-
stream path
   ForceTwoRR=-
dblquad(@forceTwoReflectedR,0,2*pi,0,pi/2);

   % Radial force due to the 2nd transmitted photon-
stream path
   ForceTwoTR=-
dblquad(@forceTwoTransmittedR,0,2*pi,0,pi/2);

   % Total radial force on the particle

ForceRadial(counter)=ForceOneRR+ForceOneTR+F
orceTwoRR+ForceTwoTR;
   counter=counter+1;
end
plot(posRadial,ForceRadial)
grid on
return
function f=opticalTrapDynamics()
% Written by Ufuk Paralı
% This function calculates (within the geometrical
optics regime) the optical trap
% dynamics of a transparent spherical particle due to
the 1st reflected and
% 1st transmitted photon-stream paths and 2nd
reflected and 2nd transmitted photon-
% stream paths of a continuous-wave TEM00
Gaussian laser beam.
% (see Figure 5 in the text)
global az
global ax
global R
global W0
global P
global n0
global ns
global lambda0
az=-5e-3; % Initial axial position of particle
ax=1e-6; % Initial radial offset of particle from center
axis of laser beam
R=5e-6; % Radius of transparent spherical particle
W0=4e-6; % Beam waist
P=200e-3; % Laser power
n0=1.0; % Refractive index of ambient
ns=1.52; % Refractive index of transparent spherical
particle
lambda0=532e-9; % Laser wavelength - m
velAxialinit=5; % Initial axial velocity - m/sec
```

```
velRadialinit=0; % Initial radial velocity - m/sec
finaltime=0.0005; % Simulation duration - sec
dt=0.00005; % Simulation time step
density=2500; % Particle density - kg/m^3
m=density*(4/3)*pi*R^3; % mass of the spherical particle - kg
g=9.8; % m/s^2
ForceWeight=m*g;
eta=1.82e-6; % Medium dynamic viscosity – kg/m.sec
drag=6*3.14*eta; % drag due to viscosity
k=drag*R; % Spring constant due to drag
timeArrayCommon=zeros(1,(finaltime/dt)+2);
accelerationArrayAxial=zeros(1,(finaltime/dt)+2);
positionArrayAxial=zeros(1,(finaltime/dt)+2);
velocityArrayAxial=zeros(1,(finaltime/dt)+2);
accelerationArrayRadial=zeros(1,(finaltime/dt)+2);
positionArrayRadial=zeros(1,(finaltime/dt)+2);
velocityArrayRadial=zeros(1,(finaltime/dt)+2);
counterCommon=1; % counter initialization
positionArrayAxial(counterCommon)=az;
positionArrayRadial(counterCommon)=ax;
velocityArrayAxial(counterCommon)=velAxialinit;
velocityArrayRadial(counterCommon)=velRadialinit;
tic; % Simulation start time
for timeCommon=0:dt:finaltime
   timeCommon

timeArrayCommon(counterCommon)=timeCommon;

ForceOneRZ=dblquad(@forceOneReflectedZ,0,2*pi,
0,pi/2);

ForceOneTZ=dblquad(@forceOneTransmittedZ,0,2*
pi,0,pi/2);

ForceTwoRZ=dblquad(@forceTwoReflectedZ,0,2*pi
,0,pi/2);

ForceTwoTZ=dblquad(@forceTwoTransmittedZ,0,2*
pi,0,pi/2);

ForceOneRR=dblquad(@forceOneReflectedR,0,2*pi,
0,pi/2);

ForceOneTR=dblquad(@forceOneTransmittedR,0,2*
pi,0,pi/2);

ForceTwoRR=dblquad(@forceTwoReflectedR,0,2*pi
,0,pi/2);

ForceTwoTR=dblquad(@forceTwoTransmittedR,0,2
*pi,0,pi/2);
   ForceDragAxial=-
k*velocityArrayAxial(counterCommon);  %Dragforce
in axial direction
   ForceDragRadial=-
k*velocityArrayRadial(counterCommon);%Dragforce
radial direction

ForceAxialNet=ForceOneRZ+ForceOneTZ+ForceTw
oRZ+ForceTwoTZ+ForceDragAxial-
   ForceWeight;

   if (positionArrayRadial(counterCommon)==0)
       ForceRadialNet=ForceDragRadial;
   else

ForceRadialNet=ForceOneRR+ForceOneTR+ForceT
woRR+ForceTwoTR+
       ForceDragRadial;
   end
   % Beginning of Velocity Verlet Algorithm

accelerationArrayAxial(counterCommon)=ForceAxia
lNet/m;

accelerationArrayRadial(counterCommon)=ForceRad
ialNet/m;


VelAxialHalfTimeStep=velocityArrayAxial(counterC
ommon)+0.5*
   accelerationArrayAxial(counterCommon)*dt;


positionArrayAxial(counterCommon+1)=positionArr
ayAxial(counterCommon)+
   VelAxialHalfTimeStep*dt;


VelRadialHalfTimeStep=velocityArrayRadial(counte
rCommon)+0.5*
   accelerationArrayRadial(counterCommon)*dt;


positionArrayRadial(counterCommon+1)=positionAr
rayRadial(counterCommon)+
   1*VelRadialHalfTimeStep*dt;

   az=positionArrayAxial(counterCommon+1);
   ax=positionArrayRadial(counterCommon+1);

ForceOneRZ=dblquad(@forceOneReflectedZ,0,2*pi,
0,pi/2);

ForceOneTZ=dblquad(@forceOneTransmittedZ,0,2*
pi,0,pi/2);

ForceTwoRZ=dblquad(@forceTwoReflectedZ,0,2*pi
,0,pi/2);
```

```
ForceTwoTZ=dblquad(@forceTwoTransmittedZ,0,2*
pi,0,pi/2);

ForceOneRR=dblquad(@forceOneReflectedR,0,2*pi,
0,pi/2);

ForceOneTR=dblquad(@forceOneTransmittedR,0,2*
pi,0,pi/2);

ForceTwoRR=dblquad(@forceTwoReflectedR,0,2*pi
,0,pi/2);

ForceTwoTR=dblquad(@forceTwoTransmittedR,0,2
*pi,0,pi/2);
   ForceDragAxial=-k*VelAxialHalfTimeStep;
   ForceDragRadial=-k*VelRadialHalfTimeStep;


ForceAxialNet=ForceOneRZ+ForceOneTZ+ForceTw
oRZ+ForceTwoTZ+
   ForceDragAxial-ForceWeight;

      if (positionArrayRadial(counterCommon+1)==0)
         ForceRadialNet=ForceDragRadial;
      else

ForceRadialNet=ForceOneRR+ForceOneTR+ForceT
woRR+ForceTwoTR+
         ForceDragRadial;
      end

accelerationArrayAxial(counterCommon+1)=ForceA
xialNet/m;

accelerationArrayRadial(counterCommon+1)=ForceR
adialNet/m;


velocityArrayAxial(counterCommon+1)=VelAxialHa
lfTimeStep+0.5*
   accelerationArrayAxial(counterCommon+1)*dt;


velocityArrayRadial(counterCommon+1)=VelRadial
HalfTimeStep+0.5*
   accelerationArrayRadial(counterCommon+1)*dt;
   % End of Velocity Verlet Algorithm
   counterCommon=counterCommon+1;
end
toc; % Simulation end time
timeArrayCommon(counterCommon)=timeCommon
+dt;
```

```
figure,plot(positionArrayRadial,positionArrayAxial),
xlabel('RadialPosition (m)'),
ylabel('Axial Position (m)'),title('Axial Position, z (m)
vs Radial Position, r (m)');

figure,plot(timeArrayCommon,positionArrayRadial),
xlabel('Time (sec)'),
ylabel('Radial Position (m)'),title('Radial Position, r
(m)');

figure,plot(timeArrayCommon,velocityArrayRadial),
xlabel('Time (sec)'),
ylabel('Radial Velocity (m/sec)'),title('Radial Velocity,
Vr (m/sec)');
return

function Ints=Intensity(ro,z)
% Written by Ufuk Paralı
% This function calculates the intensity of TEM00
Gaussian beam.
global W0
global P
global lambda0
z0=(pi*W0*W0)/lambda0; % Rayleigh range
Wz2=(W0^2)*(1+((z)/z0).^2); % Square of beam
width – (square of Eq. 11 in the text)
Ints=(2*P./(pi*(Wz2))).*exp(-2*(ro.^2)./(Wz2)); %
Intensity – see Eq. 1 in the text
return

function r1square=refCoefSquare(theta1,theta2)
% Written by Ufuk Paralı
% This function calculates the power reflectance
coefficient
% See Eq. 9 of Gauthier et al. [7].
global n0
global ns
global lambda0
r1square=(((n0*ns)^2*((cos(theta1)).^2-
(cos(theta2)).^2).^2))/((n0*ns)*((cos(theta1)).^2+
(cos(theta2)).^2)+((n0^2)+(ns^2))*(cos(theta1).*cos(t
heta2))).^2;
return

function ro2=rho2(phi,theta1,ax)
% Written by Ufuk Paralı
% This function calculates the radial distance (ρ) of a
point
% on the surface of the spherical particle from the
beam's axis.
global R
% Radial distance – see Eq. 9 in the text
ro2=((ax)^2+(2*(ax)*R*sin(theta1).*cos(phi))+(R*si
n(theta1)).^2+(R*sin(theta1)).^2).^(0.5);
return
```

```
function s=Snell(T1)
% Written by Ufuk Paralı
% Snell function
global n0
global ns
s=asin((n0/ns)*sin(T1));
return

function F1rz=forceOneReflectedZ(phi,theta1)
% Written by Ufuk Paralı
% This function calculates the axial force due to the 1st
reflected
% photon-stream path (see Figure 8) given by Eq. 22
of Gauthier et al. [7].
global az
global ax
global R
global n0
global ns
global lambda0
c=3e8;
theta2=Snell(theta1);
rhoTheta1Phi=rho2(phi,theta1,ax);
z=az-R*cos(theta1);
F1rz=(0.5/c)*n0*(1+cos(2*theta1)).*Intensity(rhoThe
ta1Phi,z).*refCoefSquare(theta1,theta2)*(R^2).*sin(2
*theta1);
return

function F1tz=forceOneTransmittedZ(phi,theta1)
% Written by Ufuk Paralı
% This function calculates the axial force due to the 1st
transmitted
% photon-stream path (see Figure 8) given by Eq. 23
of Gauthier et al. [7].
global az
global ax
global R
global n0
global ns
global lambda0
c=3e8;
theta2=Snell(theta1);
rhoTheta1Phi=rho2(phi,theta1,ax);
z=az-R*cos(theta1);
F1tz=(0.5/c)*(n0-ns*cos(theta1-
theta2)).*Intensity(rhoTheta1Phi,z).*
(1-
refCoefSquare(theta1,theta2))*(R^2).*sin(2*theta1);
return

function F2rz=forceTwoReflectedZ(phi,theta1)
% Written by Ufuk Paralı
% This function calculates the axial force due to the
2nd reflected
% photon-stream path (see Figure 8) given by Eq. 24
of Gauthier et al. [7].
global az
global ax
global R
global n0
global ns
global lambda0
c=3e8;
theta2=Snell(theta1);
rhoTheta1Phi=rho2(phi,theta1,ax);
z=az-R*cos(theta1);
F2rz=(0.5/c)*ns*(cos(theta1-theta2)+cos(3*theta2-
theta1)).*Intensity(rhoTheta1Phi,z).*
(1-
refCoefSquare(theta1,theta2)).*refCoefSquare(theta1,
theta2)*
(R^2).*sin(2*theta1);
return

function F2tz=forceTwoTransmittedZ(phi,theta1)
% Written by Ufuk Paralı
% This function calculates the axial force due to the
2nd transmitted
% photon-stream path (see Figure 8) given by Eq. 25
of Gauthier et al. [7].
global az
global ax
global R
global n0
global ns
global lambda0
c=3e8;
theta2=Snell(theta1);
rhoTheta1Phi=rho2(phi,theta1,ax);
z=az-R*cos(theta1);
F2tz=(0.5/c)*(ns*cos(theta1-theta2)-
n0*cos(2*(theta1-theta2))).*
Intensity(rhoTheta1Phi,z).*(1-
refCoefSquare(theta1,theta2)).*
(1-
refCoefSquare(theta1,theta2))*(R^2).*sin(2*theta1);
return

function F1rr=forceOneReflectedR(phi,theta1)
% Written by Ufuk Paralı
% This function calculates the radial force due to the
1st reflected
% photon-stream path (see Figure 8) given by Eq. 34
of Gauthier et al. [7].
global ax
global az
global R
global n0
global ns
```

```
global lambda0
c=3e8; % Speed of light - m/sec
z=az-R*cos(theta1); % Vertical displacement of a point – see Eq. 10 in the text
theta2=Snell(theta1);
rhoTheta1Phi=rho2(phi,theta1,ax);
F1rr=-
(n0*0.5/c)*Intensity(rhoTheta1Phi,z).*sin(2*theta1).*
refCoefSquare(theta1,theta2)*(R^2).*cos(phi).*sin(2*
theta1);
return

function F1tr=forceOneTransmittedR(phi,theta1)
% Written by Ufuk Paralı
% This function calculates the radial force due to the 1st transmitted
% photon-stream path (see Figure 8) given by Eq. 35 of Gauthier et al. [7].
global ax
global az
global R
global n0
global ns
global lambda0
c=3e8;
z=az-R*cos(theta1);
theta2=Snell(theta1);
rhoTheta1Phi=rho2(phi,theta1,ax);
F1tr=(ns*0.5/c)*Intensity(rhoTheta1Phi,z).*sin(theta1
-theta2).*
(1-
refCoefSquare(theta1,theta2))*(R^2).*cos(phi).*sin(2
*theta1);
return

function F2rr=forceTwoReflectedR(phi,theta1)
% Written by Ufuk Paralı
% This function calculates the radial force due to the 2nd reflected
% photon-stream path (see Figure 8) given by Eq. 36 of Gauthier et al. [7].
global ax
global az
global R
global n0
global ns
global lambda0
c=3e8;
z=az-R*cos(theta1);
theta2=Snell(theta1);
rhoTheta1Phi=rho2(phi,theta1,ax);
F2rr=(ns*0.5/c)*Intensity(rhoTheta1Phi,z).*(sin(3*th
eta2-theta1)-sin(theta1-theta2))*
(1-
refCoefSquare(theta1,theta2))*refCoefSquare(theta1,t
heta2)*
(R^2).*cos(phi).*sin(2*theta1);
return

function F2tr=forceTwoTransmittedR(phi,theta1)
% Written by Ufuk Paralı
% This function calculates the radial force due to the 2nd transmitted
% photon-stream path (see Figure 8) given by Eq. 37 of Gauthier et al. [7].
global ax
global az
global R
global n0
global ns
global lambda0
c=3e8;
z=az-R*cos(theta1);
theta2=Snell(theta1);
rhoTheta1Phi=rho2(phi,theta1,ax);
F2tr=(0.5/c)*Intensity(rhoTheta1Phi,z).*(n0*sin(2*(t
heta1-theta2))-ns*
sin(theta1-theta2)).*(1-
refCoefSquare(theta1,theta2)).*
(1-
refCoefSquare(theta1,theta2))*(R^2).*cos(phi).*sin(2
*theta1);
return
```

Acknowledgements

U.P. would like to acknowledge support from TÜBİTAK 1059B191401929 (The Scientific and Technological Research Council of Turkey) for his visit to Physics Department of Imperial College London. We would like to greatfully thank Prof. Roland A. Smith, Dr. Samuel Giltrap and Dr. Chris J. Price for their many helpful comments and suggestions for the numerical modeling and simulation of the optical levitation trap.

Conflicts of Interest

The authors state that they did not have conflict of interests.

References

[1] Ashkin A., Acceleration and trapping of particles by radiation pressure, *Phys. Rev.*, 24(4) (1970) 156-159.

[2] Ashkin A., Dziedzic J. M., Stability of optical levitation by radiation pressure, *Applied Physics Letters*, 24(12) (1974) 586-588.

[3] Ashkin A., Dziedzic J.M., Optical levitation in high vacuum, *Applied Physics Letters*, 28(6) (1976) 333-335.

[4] Ashkin A., Dziedzic J.M., Optical Trapping and Manipulation of Viruses and Bacteria, *Science*, 235-4795 (1987) 1517-1520.

[5] Ashkin A., Dziedzic J.M., Yamane T., Optical trapping and manipulation of single cells using infrared laser beams, *Nature*, 330-6150 (1987) 769-771.

[6] Ashkin A., Forces of a single-beam gradient laser trap on a dielectric sphere in the ray optics regime, *Biophysical Journal*, 61(2) (1992) 569-582.

[7] Gauthier R.C., Wallace S., Optical levitation of spheres: analytical development and numerical computations of the force equations, *J. Opt. Soc. Am. B.*, 12(9) (1995) 1680-1686.

[8] Kim S.B., Kim S.S, Radiation forces on spheres in loosely focused Gaussian beam: ray-optics regime, *J. Opt. Soc. Am. B.*, 23(5) (2006) 897-903.

[9] Ganic D., Gan X., Gu M., Optical trapping force with annular and doughnut laser beams based on vectorial diffraction, *Optics Express*, 13(4) (2005) 1260-1265.

[10] Price C.J., Donnelly T.D., Giltrap S., Stuart N.H., Parker S., Patankar S., Lowe H.F., Drew D., Gumbrell E.T. and Smith R.A., An in-vacuo optical levitation trap for high-intensity laser interaction experiments with isolated microtargets, *Review of Scientific Instruments*, 86(3) (2015) 033502.

[11] Sakai K. and Noda S., Optical trapping of metal particles in doughnut-shaped beam emitted by photonic-crystal laser, *Electronics Letters*, 43(2) (2007) 107-108.

[12] Zhang Y., Li Y., Qi J., Cui G., Liu H., Chen J., Zhao L., Xu J., Sun Q., Influence of absorption on optical trapping force of spherical particles in a focused Gaussian beam, *J. Opt. A: Pure Appl. Opt.*, 10(8) (2008) 085001.

[13] Shahabadi, V., Ebrahim M., Daryoush A., Optimized anti-reflection core-shell microspheres for enhanced optical trapping by structured light beams, *Scientific Reports*, 11(1) (2021) 1-10.

[14] Kalume, A., Chuji W., Yong-Le P., Optical-Trapping Laser Techniques for Characterizing Airborne Aerosol Particles and Its Application in Chemical Aerosol Study, *Micromachines*, 12(4) (2021) 466.

[15] Komoto S. et al., Optical Trapping of Polystyrene Nanoparticles on Black Silicon: Implications for Trapping and Studying Bacteria and Viruses, *ACS Applied Nano Materials*, 3(10) (2020) 9831-9841.

[16] Barton J.P., Alexander D., Schaub S.A., Theoretical determination of net radiation force and torque for a spherical particle illuminated by a focused laser beam, *J. Appl. Phys*., 66(10) (1989) 4594-4602.

[17] Kim J.S., Lee S.S., Scattering of laser beams and the optical potential well for a homogeneous sphere, *J. Opt. Soc. Am*., 73(3) (1983) 303-312.

[18] Barton J.P., Alexander D., S. A. Schaub, Internal and near-surface electromagnetic fields for a spherical particle irradiated by a focused laser beam, *J. Appl. Phys*., 64(4) (1988) 1632-1639.

[19] Ashkin A., Forces of a single-beam gradient laser trap on a dielectric sphere in the ray optics regime, *Biophys. J.,* 61(2) (1992) 569-582.

[20] Chang S., Lee S.S., Optical torque exerted on a homogeneous sphere levitated in circularly polarized fundamental-mode laser beam, *J. Opt. Soc. Am. B.*, 2(11) (1985) 1853-1860.

[21] Ashkin A., Trapping of atoms by resonance radiation pressure, *Phys. Rev. Lett*., 40(12) (1978) 729-732.

[22] Ashkin A, Dziedzic J.M., Bjorkholm J.E., Chu S., Observation of a single-beam gradient force optical trap for dielectric particles, *Optics Lett.,* 11(5) (1986) 288-290.

[23] Zhang Y., Li Y., Cui G., Liu H., Chen J., Xu J., Sun Q., Transverse optical trapping of spherical particle with strong absorption in a focused Gaussian beam, *Proc. of SPIE*, 6832-68320K-1 (2008).

[24] Usman A., Ching W., Masuhara H., Optical trapping of nanoparticles by ultrashort laser pulse, *Science Progress*, 96(1) (2013) 1-18.

[25] Choudhary D., Mossa A., Jadhav M., Cecconi C., Bio-molecular Applications of Recent

Developments in Optical Tweezers, *Biomolecules*, 9(1) (2019) 23.

[26] Hempston D., Vovrosh J., Winstone G., Rashid M., Ulbricht H., Force sensing with an optically levitated charged nanoparticle, *Appl. Phys. Lett*., 111(13) (2017) 133111.

[27] Monteiro F., Ghosh S., Fine A.G., Moore D.C., Optical levitation of 10 nanogram spheres with nano-g acceleration sensitivity, *Phys. Rev. A*., 96(6) (2017) 063841.

[28] Kim J., Shin J.H., Stable, Free-space Optical Trapping and Manipulation of Sub-micron Particles in an Integrated Microfluidic Chip, *Scientific Reports*, 6 (2016) 33842.

[29] Vovrosh J., Rashid M., Hempston D., Bateman J., Paternostro M., H. Ulbricht, Parametric Feedback Cooling of Levitated Optomechanics in a Parabolic Mirror Trap, *J. Opt. Soc. Am. B.,* 34(7) (2017) 1421-1428.

[30] Thorlabs Optical Tweezers Microscope System, Trapping Theory & Force Analysis. Available at: https://www.thorlabs.com/newgrouppage9.cfm?objectgroup_id=12442. Retrieved 2020.

[31] Wilson K.R., Swope W, Andersen H., Berens P., A computer simulation method for the calculation of equilibrium constants for the formation of physical clusters of molecules: Application to small water clusters, *J. Chem. Phys*., 76(1) (1982) 637-649.

[32] Saleh B.E.A., Teich M.C., Fundamentals of Photonics, 2nd ed., New Jersey: John Wiley & Sons, (2007)

[33] Galvez E.J., Gaussian beams in the optics course, *Am. J. Phys*., 74(4) (2006) 355-361.

[34] Beijersbergen M.W., Allen L., Veen H.O., Woerdman J.P., Astigmatic laser mode converters and transfer of orbital angular momentum, *Optics Communications*, 96(3) (1993) 123-132.

[35] Zauderer E., Complex argument Hermite-Gaussian and Laguerre-Gaussian beams, *J. Opt. Soc. Am. A.,* 3(4) (1986) 465-469.

[36] Gradshteyn I.S., Ryzhik I.M., Table of Integrals, Series and Products, 8th ed., California: Elsevier, (2015)